Rigid unit modes in framework silicates

MARTIN T. DOVE[1], VOLKER HEINE[2] AND KENTON D. HAMMONDS[1]

[1] Department of Earth Sciences, University of Cambridge, Downing Street, Cambridge CB2 3EQ, UK
[2] Cavendish Laboratory, University of Cambridge, Madingley Road, Cambridge CB3 OHE, UK

Abstract

We describe a model for framework silicates in which the SiO_4 (and AlO_4) tetrahedra are treated as perfectly rigid and freely jointed. From this model we are able to identify low-energy modes of distortion of the structure, which we call Rigid unit modes. These modes can act as soft modes to allow easy distortions at phase transition. We discuss three forces that will operate at a phase transition in conjunction with the candidate soft modes to determine which of the rigid unit modes will actually precipitate a phase transition, and illustrate these ideas by detailed discussions of the phase transitions in quartz, leucite and cristobalite. The model can also be used to estimate the transition temperature, and the theory highlights an important role for the stiffness of the tetrahedra.

KEYWORDS: rigid unit modes, phase transitions, quartz, leucite, cristobalite.

The paradox of framework aluminosilicates

THOSE of us who come into Mineralogy from other disciplines are frequently struck by a paradox posed by framework aluminosilicates: despite the fact that silicates are amongst the strongest and most stable of materials, there are a number of intriguing theoretical problems associated with their structural stability. One is that aluminosilicates are riddled with phase transitions. Another is that aluminosilicates have considerable chemical flexibility, as they are able to form solid solutions over wide compositional changes. Aluminosilicates sometimes have unusual thermal expansion properties, and zeolites have a number of industrially important chemical properties. So what is going on with these aluminosilicate frameworks?

It turns out that, unlike engineering frameworks, the frameworks built from linkages of perfectly rigid SiO_4 and AlO_4 tetrahedra are not themselves perfectly rigid. Instead, they can have some internal degrees of freedom of distortion, which give rise to low-frequency phonon modes that can propagate with no distortions of the tetrahedra. We call these Rigid Unit Modes (RUMs), and their existence provides natural candidates for the soft modes that typically drive displacive phase transitions (Dove *et al.*, 1992, 1993, 1995*a*). The idea has its roots in the geometrical polyhedral tilting models of Megaw (1973) and Hazen and Finger (1982).

The existence of RUMs in an aluminosilicate framework structure is more subtle a point than might initially be imagined. Each tetrahedron has 6 degrees of freedom, and each linked corner has three constraint equations that prevent the linkage from splitting. Thus the number of constraints per tetrahedron is ½ (from a sharing between two tetrahedra of the constraints on a single linkage) × 4 (the number of corners of a tetrahedron), which is the same as the number of degrees of freedom: the numbers of constraints and degrees of freedom are exactly matched. However, we have shown elsewhere (Dove *et al.*, 1992; Giddy *et al.*, 1993) that it is possible for some of these constraints to be degenerate, i.e. not independent. A simple example of a degenerate constraint is shown in Fig. 1. This is a function of symmetry rather than topology, and as a result the high-temperature phases of framework silicates can have some modes of distortion that do not occur in corresponding low-temperature phases.

A computational method: the split-atom method

We have developed a computational method to allow us to determine the complete RUM spectrum for any framework silicate (Giddy *et al.*, 1993; Hammonds *et*

Mineralogical Magazine, December, Vol. 59, pp. 629–639

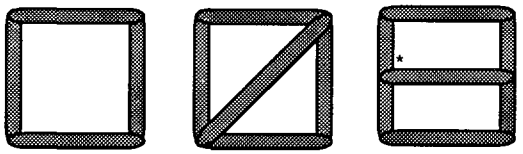

$F = 12$ $C = 8$ | $F = 15$ $C = 12$ | $F = 15$ $C = 11$

FIG. 1. A two-dimensional example of the effect of symmetry on the number of independent constraints. The three structures are formed by bars hinged at common corners. Each bar has 3 degrees of freedom: 2 translations and 1 rotation, so the total number of degrees of freedom for the bars in each structure, F, is simply equal to 3 × the number of bars. At each corner there are two constraint equations, forcing the hinge points of two jointed bars to have the same x and y coordinates. Therefore, the number of constraint equations associated with each structure, C, is simply equal to 2 × the number of corners. The resultant number of degrees of freedom for each structure is $F - C$. Three of these will be the rigid-body motions of the structure, two translations and one rotation. In the left-hand structure, there is an additional degree of freedom, the possibility to shear the structure. This degree of freedom is lost in the middle structure as a result of the extra constraints imposed by the cross-brace bar. However, the right-hand structure presents an interesting contradiction, for although it has the same number of constraints as the middle structure it can clearly also be sheared. The solution to this problem is to note that the two constraints associated with the joint marked * can be replaced by the single constraint that the middle bar should be parallel to the top and bottom bars. This then reduces the value of C by 1.

al., 1994). The heart of the method involves identifying each tetrahedron as an individual rigid unit. The oxygen atoms that are shared between two tetrahedra are split into two, which we call the split atoms. In our approach two split atoms are then kept together by a strong harmonic force. The RUMs will be the vibrational modes in which the tetrahedra can move without the split atoms becoming separated, and the modes that require distortions of the tetrahedra will, in the split-atom representation, be the modes in which the split atoms are forced to separate. To first order, the strength of the split-atom force constant can be related to the stiffness of the tetrahedra.

The dynamical equations of the split-atom method can be cast into the formalism of molecular lattice dynamics (Pawley, 1972), and we have modified a computer program to work with the split-atom method (Giddy *et al.*, 1993; Hammonds *et al.*, 1994). The RUMs are the phonon modes that are calculated with zero frequency. We have found that it is sometimes useful to add a nearest-neighbour Si–Si interaction, which attempts to model a constraint that will keep the Si–O–Si bond angle fixed at an ideal value (Hammonds *et al.*, 1994). The results of a RUM analysis for a few selected systems have been given by Dove *et al.* (1995*a*), and discussed in more detail by Hammonds *et al.* (1995).

Experimental evidence

There is a good body of experimental data, direct and indirect, that confirms the idea of the existence of rigid unit modes as low-frequency phonons. The most direct observation of RUMs can be obtained by inelastic neutron spectroscopy. The case of quartz has been documented in detail elsewhere (Berge *et al.*, 1986; Bethke *et al.*, 1987; Dolino *et al.*, 1989, 1992; Vallade *et al.*, 1992), and the experimental picture has been reproduced by molecular dynamics simulations (Tautz *et al.*, 1991). The other important example in which RUMs have been observed by inelastic neutron spectroscopy is leucite (Boysen, 1990). Our calculations for leucite using the split-atom method have shown that there are RUMs along ⟨110⟩. The relevant inelastic neutron scattering data are shown in Fig. 2, where the mode frequencies are plotted as a function of wave vector (Boysen, 1990). The low-frequency modes that correlate with the RUMs are highlighted, although not all the RUMs have been measured (and indeed the results shown in Fig. 2 are only tentative). One point to note is that the frequency of a mode is a RUM at one wave vector but not at any other point along a given direction in reciprocal space will increase rapidly when moving along this direction. This is seen for leucite in Fig. 2: some of the components of the triply-degenerate RUM at $\mathbf{k} = 0$ are not RUMs for wave vectors along the two directions in reciprocal space shown in this figure, and their frequencies rapidly rise on moving away from this wave vector.

Low-frequency phonons can also be observed as diffuse scattering in electron or X-ray diffraction. The streaks of diffuse electron diffraction found in cubic β-cristobalite (Hua *et al.*, 1988; Welberry *et al.*, 1989; Withers *et al.*, 1989) are in exact agreement with our calculations of the RUM spectrum (Dove *et al.*, 1992, 1993, 1995*a*), which predict the existence of RUMs with wave vectors of the form $\{\xi,\xi,\zeta\}$. More recently patterns of diffuse electron diffraction in the high-temperature phase of tridymite (Withers *et al.*, 1994) have also been found to be in perfect agreement with the calculated RUM spectrum (Dove *et al.*, 1995*b*). This is actually a significant test of the

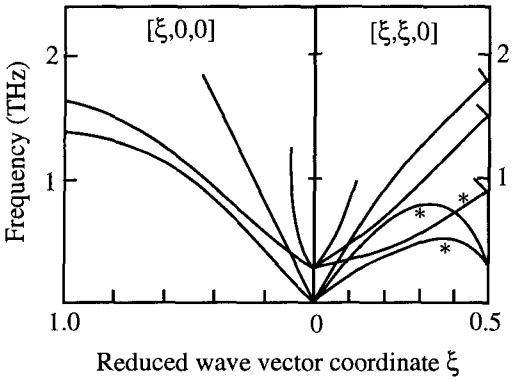

FIG. 2. The low-frequency phonon dispersion curves of leucite determined by inelastic neutron spectroscopy by Boysen (1990). The phonon branches indicated by * are identified as the RUMs. The optic mode at $\mathbf{k} = 0$ is the T_{1g} RUM. Not all the phonon branches have been measured, and the interpretation of the measurements that are available are only tentative. Nevertheless, the low-frequency modes along [110] can clearly be interpreted within the RUM model, and the way that some phonon branches come in steeply towards the wave vector at which they become a RUM is characteristic behaviour. Note the anticrossing between the upper transverse acoustic mode and an optic mode (Dove, 1993).

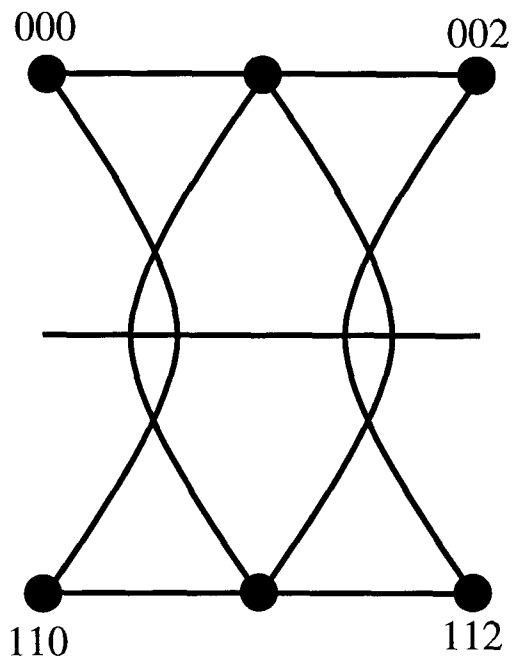

FIG. 3. Section of the RUM surface of tridymite in reciprocal space. There are RUMs at each wave vector on the curved surface and on each line, which are seen in diffuse electron diffraction measurements (Withers *et al.*, 1995). The large circles are reciprocal lattice vectors. This pattern is repeated throughout this section of reciprocal space.

RUM model. Streaks of diffuse scattering were easily explained as arising from the existence of RUMs in symmetry planes in reciprocal space. However, the diffraction patterns also showed a strong curved surface of diffuse scattering, which passed through some special symmetry points but which mostly followed a general curve in reciprocal space. This curved surface has been exactly reproduced by our split-atom calculations, and is shown in Fig. 3. Confirmation that these patterns of diffuse scattering arise from phonon modes rather than static disorder comes from the fact that most of the scattering disappears completely on cooling into the low-temperature phases, consistent with our split-atom calculations for the low-temperature phases.

A dramatic demonstration of the existence of low-frequency phonons in β-cristobalite that vanish on cooling into the α-phase was obtained by inelastic neutron spectroscopy with powder samples (Swainson and Dove, 1993*a*). These results were reproduced by calculations of the vibrational density of states by molecular dynamics simulation (Swainson and Dove, 1995).

Rigid unit modes and displacive phase transitions

What drives a displacive phase transition?

We have identified three forces that are important in driving a phase transition. The first arises from the polarisability of the oxygen ions, leading to the classical dispersive (or Van der Waals) interactions that fall off as $-1/(\text{distance})^6$. When integrated over the whole crystal, i.e. over distances to infinity, the energy involved is not insignificant, and scales as 1/density. Thus this interaction always drives a system to its highest density allowed by the short-range repulsive interactions. The high-temperature phases are always in a minimum density configuration, so the phase transition will always lead to an increase in density and hence a lowering of the dispersive energy. Thus the dispersive energy always acts as a force to drive a phase transition from a high-symmetry phase to one of lower symmetry and higher density. It is useful to express this in terms of an effective inward pressure. If we characterise the

distortion that accompanies a phase transition by an order parameter Q, the driving energy for the transition is $\Delta U \propto -Q^2$. The volume change that accompanies the phase transition is given as $\Delta V \propto -Q^2$. These are related by the effective pressure: $P = \Delta U/\Delta V$.

The second driving force is the short-range inward pull that a cation in a cavity exerts on its neighbouring oxygen anions. Cavities are reasonably common in open framework structures. This inward pull will always try to force a collapse of the cavity around the cation and thereby drive a structure into a lower symmetry phase.

The third force is associated with the preference for the Si–O–Si bond angles to be around 145–150° (Lasaga and Gibbs, 1988). In cristobalite, where the bond angles in the ideal structure of the β-phase are 180, this force drives the transition to the ordered α-phase with more favourable bond angles (see below). On the other hand, many high-symmetry structures, such as quartz and leucite, already have Si–O–Si bond angles with reasonable values, and some RUMs will actually cause these angles to deviate away from their most favourable angles. When we calculate the RUM spectrum for a given structure with the inclusion of the Si–Si force constant, we generally find that only a few of the RUMs are calculated with zero frequency. Thus in some cases the Si–O–Si bond angle force can oppose a distortion, but in other cases can drive the phase transition.

Finally, noting that the energy required to distort a tetrahedron is of higher energy than any of these processes, the displacive phase transitions found in aluminosilicate framework structure will be those allowed by RUM distortions. Which RUM actually operates will usually depend on the balance of these three forces (although in some cases other forces, such as arise from electronic instabilities, may come into play).

Quartz

The RUM model was initially developed with respect to the phase transitions in quartz. Megaw (1973) and Grimm and Dorner (1975) pointed out that many features of the classical α–β phase transition can be explained using a simple geometric model in which the SiO_4 tetrahedra move as rigid bodies (Fig. 4). These ideas were extended by Berge *et al.* (1986) and Vallade *et al.* (1992) in order to explain the existence

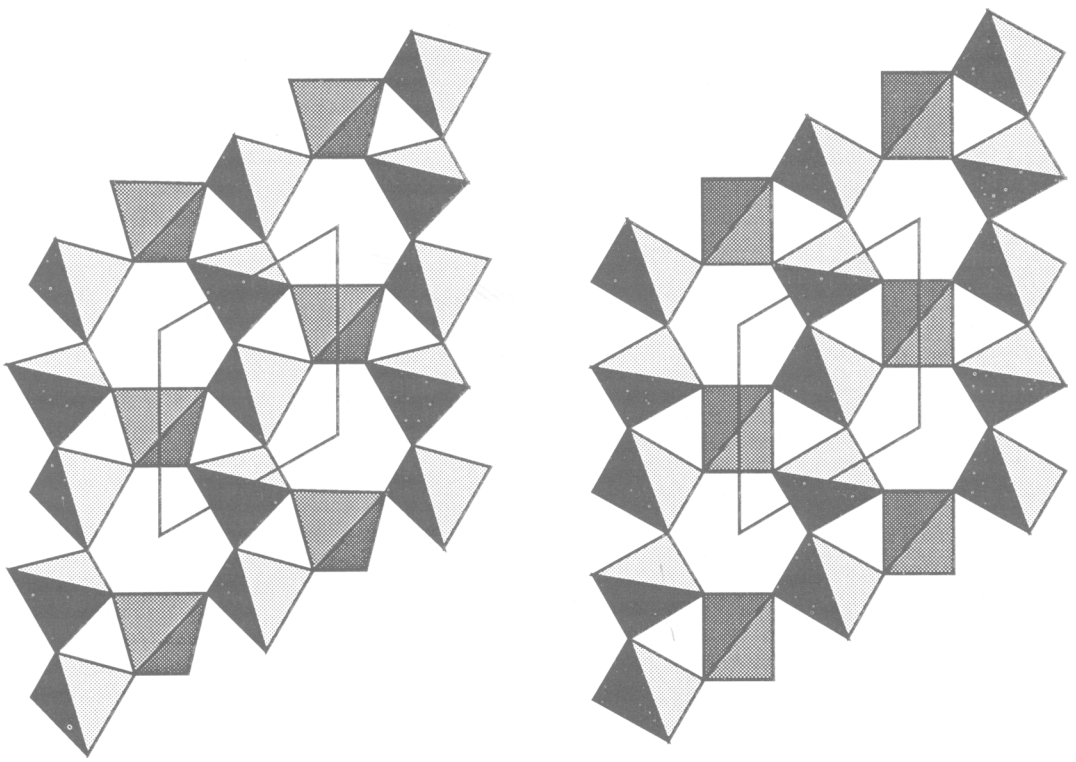

FIG. 4. Crystal structures of the α (left) and β (right) phases of quartz, with SiO_4 tetrahedra shown as shaded rigid units. The two crystal structures are drawn with the same unit cells, viewed down a common [001] direction.

of the intermediate incommensurate phase. Not only did the RUM model provide a description of the incommensurate phase, it also provided an explanation for its existence. The key point is that the existence of a line of RUMs along the [100] directions forces the incommensurate instability to occur on cooling before the transition to the b-phase can occur. The details have been confirmed by inelastic neutron scattering experiments (Berge *et al.*, 1986; Vallade *et al.*, 1992) and molecular dynamics simulations (Tautz *et al.*, 1991). From this work the phase transition in quartz is clearly seen as a classic soft-mode phase transition, in agreement with many other results but in contradiction to some assertions that the transition involves an order–disorder mechanism.

In β-quartz there are RUMs for wave vectors along all the main symmetry directions. We have calculated that the dispersive energy provides a inward pressure of $P = 140$ kbar. Since there is a clear driving force for a phase transition, we are posed with the question as to why the α–β phase transition arises from an instability with zero wave vector, rather than from a wave vector at one of the points on the surface of the Brillouin zone? When we calculate the RUM spectrum for β-quartz with the Si–Si force, we find that the only RUM that retains its zero frequency is the RUM at zero wave vector. Thus only for this specific distortion does the force associated with the Si–O–Si bond angle not oppose the phase transition, and this provides a possible explanation of why this instability is favoured over all others.

Leucite, $KAlSi_2O_6$

Leucite undergoes a cubic–tetragonal phase transition at ~940 K (Fig. 5). A number of mechanisms have been invoked to explain this phase transition, including Al/Si ordering (which seems unlikely, as we have discussed elsewhere (Dove *et al.*, 1992)) and K-site ordering. The high-temperature phase is cubic, space group *Ia3d*. The low-temperature phase has space group $I4_1/a$, which can be derived from the cubic phase by an instability of T_{1g} symmetry and zero wave vector, or by a two stage process involving an instability of E_g symmetry in the cubic phase to produce a tetragonal phase of space group $I4_1/acd$, followed by an instability of A_{2g} symmetry in this intermediate phase, both of zero wave vector (Boysen, 1990; Palmer, 1990). There is experimental evidence for the existence of this intermediate phase, but the two pathways are not dissimilar since an A_{2g} mode in the intermediate phase forms part of a T_{1g} mode in the cubic phase. The questions we have, particularly in view of the large number of ways of distorting the cubic phase, is what exactly happens and why?

Our RUM calculations for the cubic phase of leucite show the existence of 4 RUMs along the ⟨110⟩ directions, and at zero wave vector there are 8 RUMs. These are the $A_{2g} + A_{2u} + T_{1g} + T_{1u}$ modes, where the T_{1u} modes are the three acoustic modes. There are no E_g modes, which would be necessary if the transition from *Ia3d* to $I4_1$ / *acd* involved an optic instability. However, the acoustic modes generate

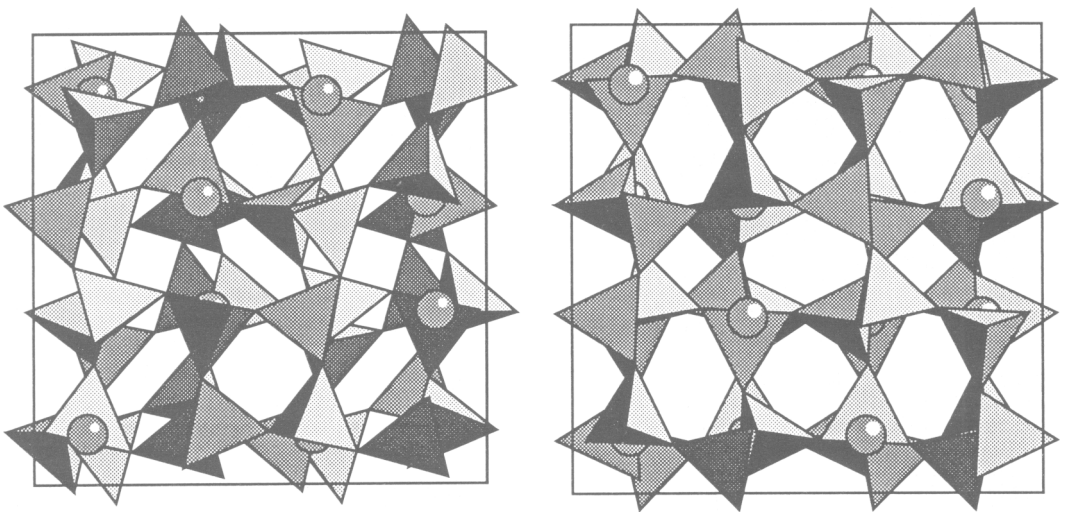

FIG. 5. Crystal structures of the tetragonal (left) and cubic (right) phases of leucite, with SiO_4 and AlO_4 tetrahedra shown as shaded rigid units. The two crystal structures are drawn with the same unit cells, viewed down a common [001] direction.

strains of E_g symmetry. The change in space group from $Ia3d$ to $I4_1/acd$ is allowed to be a proper ferroelastic phase transition, in which the primary mechanism is a soft acoustic mode generating a shear strain of the structure. Thus the first stage in the phase transition will involve the condensation of the soft acoustic modes. In such transitions we often encounter the classic Chicken and Egg question — does the ferroelastic instability follow from an acoustic mode softening, or does the acoustic mode soften as a result of another instability. In this case we can assert that there is a natural soft acoustic mode for the phase transition, and no other RUM distortions of the same symmetry. This instability is therefore generated by an acoustic mode softening, and the corresponding order parameter is a shear strain, rather than the shear strain coming in through coupling to another order parameter. Our RUM calculations for the intermediate phase show that there are RUMs of symmetry $A_{2g} + A_{2u} + E_u + B_{1g} + B_{1u}$, where $A_{2u} + E_u$ are the acoustic modes. The optic RUMs of the cubic phase transform as $A_{2g} \rightarrow B_{1g}$, $A_{2u} \rightarrow B_{1u}$ and $T_{1g} \rightarrow A_{2g} + E_g$, but the E_g mode in this last case is not a RUM in the intermediate phase. The second stage of the phase transition, the transformation from $I4_1/acd$ to $I4_1/a$, involves the condensation of the A_{2g} optic RUM. It is not clear whether in the cubic phase the condensation of the E_g strain mode and the A_{2g} component of the T_{1g} optic RUM are independent, or whether the softening T_{1g} optic RUM precipitates the softening of the acoustic mode (the relevant acoustic RUM along ⟨110⟩ has the same symmetry as one of the components of the T_{1g} mode). In the latter case, there may be some mixing of eigenvectors, but the point is that the cubic phase is inherently elastically soft without being driven so through coupling to a softening optic instability. Further investigations by inelastic neutron spectroscopy on single crystals over a range of temperatures and by Raman scattering, particularly in the frequency regime below 1 THz, would certainly help confirm the overall picture and provide information about the link between the optic and acoustic RUM instabilities.

We now consider the driving force for this phase transition. In order to draw comparison with quartz we have performed a simple lattice energy minimisation calculation of SiO_2 starting in the $I4_1/a$ leucite structure, using the interatomic potential model for silica of Sanders *et al.* (1984). The lattice energy is minimised when the structure reverts back to the high-symmetry $Ia3d$ structure. Thus the dispersive energy does not provide a sufficient driving force for this phase transition, even though the volume change associated with the phase transition is quite large. Instead, the Si–O–Si bond angles have more favourable values in the cubic phase, and the forces these generate are stronger than the dispersive forces. This is reinforced by our RUM calculations on the cubic phase with the Si–Si potential: we find that none of the RUMs retain their zero frequency with this interaction turned on. Thus the inward pull of the K^+ cations is essential to drive the phase transition. Now we ask why the transition involves an instability at zero wave vector rather than at [½½0], which is the other candidate wave vector where RUMs are found. Moreover, why is the T_{1g} RUM preferred over the other RUMs at zero wave vector? The answers are suggested by the RUM calculations with the Si–Si potential turned on — of the optic RUMs, the T_{1g} RUM at $\mathbf{k} = 0$ is the one that distorts the Si–O–Si bond angle the least, so that the opposing force associated with this bond angle is the lowest.

We therefore conclude that in leucite there is a two-stage transition from the high-temperature cubic phase to the low-temperature tetragonal phase. The first involves a soft acoustic instability resulting in a proper ferroelastic phase transition, and the second involves the softening of an optic RUM. The basic picture has been confirmed in part by the inelastic neutron scattering measurements of Boysen (1990), discussed earlier (Fig. 2). Thus the phase transitions in leucite are classical soft mode phase transitions, and there is no need to invoke mechanisms based on alternative ordering processes.

Finally is interesting to note that the tables of Stokes and Hatch (1988) show that there are 133 possible phase transitions from the cubic $Ia3d$ phase of leucite, involving a wide range of instabilities and possible low-temperature phases. Our RUM analysis has allowed us to understand why out of this long list of possibilities the leucite structure transforms in the particular way it does.

Cristobalite

The phase transition in cristobalite can be cast in the language of soft-modes by noting that the symmetry change at the α–β transition (Fig. 6) involves an unstable RUM with wave vector [100] on the surface of the Brillouin zone of the b-phase (Hatch and Ghose, 1991). However, the phase transition has more of the nature of an order–disorder transition. The ideal cubic structure of the β-phase has linear Si–O–Si bonds, which are not energetically favourable. Structure refinements (Schmahl *et al.*, 1992), NMR studies (Phillips *et al.*, 1993), and molecular dynamics simulations (Swainson and Dove, 1993*a*, 1995) of the β-phase suggest that the Si–O bonds are oriented at quite a large angle ($\sim 17°$) to the expected orientations in the ideal cubic structure, ⟨111⟩. If this can be accomplished by some mechanism in which the tetrahedra can tilt as rigid

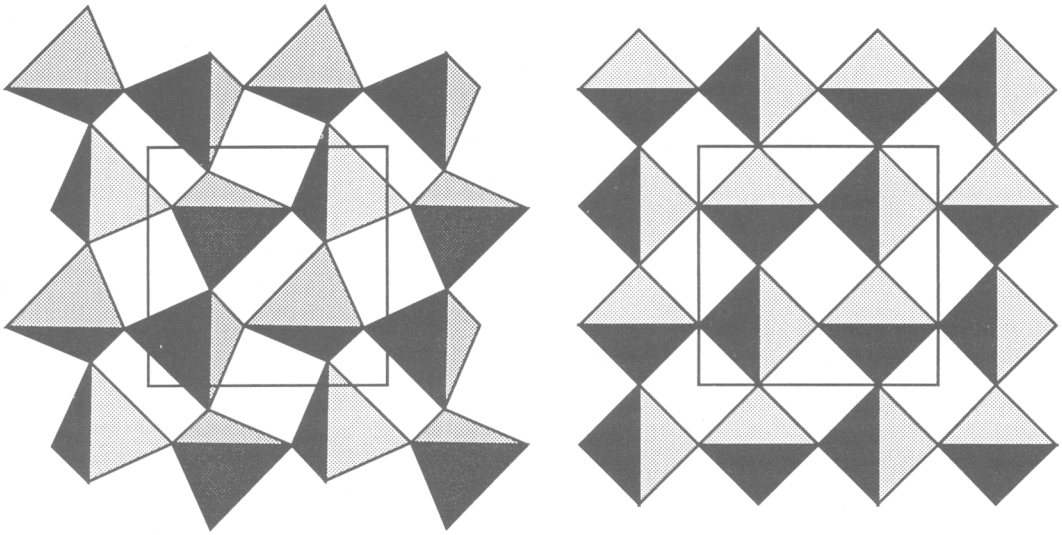

FIG. 6. Crystal structures of the α (left) and β (right) phases of cristobalite, with SiO_4 tetrahedra shown as shaded rigid units. The two crystal structures are drawn with the same unit cells, viewed down a common [001] direction.

bodies, the energy could be considerably lowered as a result of the Si–O–Si bond angles coming closer to their ideal values with no cost associated with the high-energy distortions of the tetrahedra. The cubic structure will then necessarily be disordered. There are two ways in which this might be accomplished. Conceptually, the simplest is to assume that the β-phase consists of domains of a structure of lower symmetry in which the tetrahedra are rotated to give favourable Si–O–Si bond angles. Hatch and Ghose (1991) have suggested that the domains have the structure of the α-phase, whereas Wright and Leadbetter (1975) have suggested an alternative structure. Both proposed structures correspond to RUM distortions of the ideal cubic structure (Swainson and Dove, 1993*b*). The symmetry of the cubic phase is preserved as a result of static disorder, in which the long-range order of the β-phase is obtained by averaging over domains of different orientation. The second way to obtain disorder is for the tetrahedra to be dynamically disordered, with continuous reorientational motions of the tetrahedra (Swainson and Dove, 1993*a*). This can be accomplished as the result of the operations of planes of RUMs in reciprocal space. At any instance a disordered arrangement can be obtained as a linear superposition of RUMs with different phases, including the RUMs that give rise to the two domain structures outlined above. This linear combination will evolve with time, leading to dynamic disorder. Domains of lower-symmetry structures can appear as fluctuations within this process, but they will be mixed in with all possible fluctuations. This is discussed in more detail elsewhere (Hammonds *et al.*, 1995).

What determines the transition temperature?

Renormalised phonon theory

The simplest version of renormalised phonon theory gives an expression for the transition temperature, T_c:

$$k_B T_c = -\omega_0^2 / \sum_k (\alpha_k / \omega_k^2) \qquad (1)$$

where ω_0 is the frequency of the soft mode at $T = 0$ K (and hence is an imaginary quantity), ω_k is the frequency of any other phonon mode labelled as k, and α_k is the coefficient of the fourth-order anharmonic interaction between the phonon k and the soft mode (Dove, 1993). A calculation for quartz gives a value for T_c which is about 1.5 times the right answer (Dove and Heine, 1995). The errors reflect the approximations used in the application of renormalised phonon theory. The interesting point is that the magnitudes of the individual values of α_k/ω_k^2 are large but equally distributed over positive and negative values. Thus most terms in the denominator in equation (1) cancel, and it has a value that is much smaller than the maximum values of $|\alpha_k/\omega_k^2|$. Given that the final value of the denominator will be a very sensitive balance between large positive and negative terms, the final

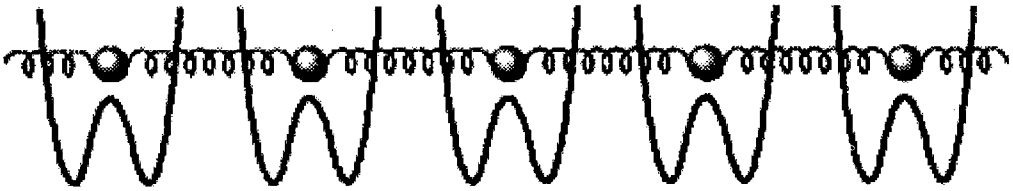

FIG. 7. A simple model of a monatomic crystal that displays a phase transition. The atoms interact with nearest neighbours by harmonic forces, represented by the springs. Each atom also oscillates in a local double-well potential, represented by the curves at each lattice point. The local potentials are a way of representing the effects of the rest of the crystal.

value of T_c might be expected to be quite chaotic. Indeed, it could be infinite. We will see below that the RUM picture allows us to understand the resultant values of T_c.

Another approach towards the transition temperature

Fig. 7 shows a simple model that has often been used to gain insights into the basic phenomena at a phase transition. A set of atoms are linked by simple harmonic forces, and each atom vibrates in its own 'double-well' potential. Fig. 7 shows a one-dimensional version of the model, but it is easily generalised to three dimensions, although it is most easily used if there is still only one variable per atom. The simple renormalised phonon theory described above can be applied exactly to this model. The harmonic force constant is J, and the potential double-well is described as $-\frac{1}{2}au^2 + \frac{1}{4}bu^4$, where u is the displacement of the atom. We note that the minima of the double-well potentials occur at $\pm u_0 = \pm a/b$, the transition temperature is given from renormalised phonon theory in the limit $J \gg a$ as (Bruce and Cowley, 1981; Sollich *et al.*, 1994)

$$k_B T_c \propto J u_0^2 \qquad (2)$$

We now use the proportional sign since the exact result is modified by well-understood but uninteresting geometric terms. To express equation (2) in the symbols of equation (1), we note that ω_k^2 is determined by J, $\alpha_k = b$ for all values of k, and $\omega_0^2 = -a$.

We can relate this model to our RUM system by identifying the displacement u as a generalised rotation/translation of a tetrahedron, and the interaction between tetrahedra J as proportional to the stiffness of the tetrahedra: this point has been discussed in detail elsewhere (Dove *et al.*, 1992, 1993, 1995*a*). The important point that follows from equation (2) is that the transition temperature is determined by only two factors. The first is the stiffness of the tetrahedra, and the second is the maximum distortion as determined by local repulsive forces.

Using a geometry appropriate to quartz, and taking account of the existence of RUMs along all the main symmetry directions, we have calculated a value for T_c of around 1000 K, with a realistic estimate for J, but subject to a fairly-high level of uncertainty (Dove *et al.*, 1995*a*). The key point here is not the exact value we calculate, but the fact that the simple model, in which account is taken of only one phonon branch, gives a result that is similar to for the full calculation that takes everything into account.

We should remark on the significance of the limit $J \gg a$. By mapping the RUM model onto the simple model, this condition follows from the fact that the stiffness of the tetrahedra is much larger than any other force constant, and certainly higher than the driving forces for the phase transition that will form the local double-well potentials. From a detailed study of the model (Bruce and Cowley, 1981) we know that the limit $J \gg a$ provides the condition that the order parameter for the phase transition, Q, has the temperature dependence $Q = \langle u \rangle \propto (T_c - T)^{\frac{1}{2}}$. This provides some validation for the successful application of Landau theory to these phase transitions.

What do we learn from the comparison of the two models?

It is interesting to note that the two models described above give similar results. The results are not perfect, as a result of approximations inherent in the model, but they are close enough to the actual value of T_c to give us confidence that the models have captured some essential elements of the truth. The principal difference between the two models is that the full model takes explicit account of all 27 phonon branches, whereas the simple model contains only one phonon branch. In the first case it turned out that

the contributions of all the phonon modes to the denominator in the calculation of T_c were largely self-cancelling, leading to the question of why the resultant value of T_c is not nearer in value. This is answered by the results of the simple model. In the simple model a single anharmonic force constant operates for all wave vectors of the phonon branch. This prevents any cancellation of the terms in the denominator of equation (2). It appears as if the phonon branch containing the soft mode in quartz operates in exactly the same way. The contributions from the other branches cancel out, but the contributions from the important phonon branch do not, and these then determine the value of the transition temperature.

We can then directly apply the insights gained from the simple model to the phase transitions in aluminosilicates. The first is that the transition temperature is determined by the stiffness of the tetrahedra and the maximum distortion of the structure in the low-temperature phase. The second is that the phase transitions in aluminosilicates operate near the soft-mode limit where Landau theory is applicable.

Relationship to the effects of chemical composition

Equation (2) contains an important implication for materials with variable chemical content, for example the alkali feldspars $K_xNa_{1-x}AlSi_3O_8$, which undergo a monoclinic–triclinic displacive phase transition. As an aside, we point out that our RUM analysis for this transition shows that it is driven by an elastic softening rather than an optic instability (Hammonds *et al.*, 1995). In the alkali feldspars, we expect the stiffness of the tetrahedra, and hence the value of J in equation (2), to be independent of the K content x. The major effect of replacing the Na cations by the larger K cations will be to reduce the maximum distortion possible, since this is controlled by the extent to which the aluminosilicate framework can collapse about the alkali cation site. Thus from equation (2) we expect that as the maximum distortion, represented by u_0^2, decreases with x, so also will the transition temperature. This result is not necessarily intuitive, for it might be argued that the effect of increased K content would be to stiffen the whole structure and therefore to raise the transition temperature. We have taken data for the alkali feldspar from Carpenter (1988). In this case the distortion associated with the phase transition is characterised by $\cos^2\alpha^*$, where α^* is one of the angles in the reciprocal unit cell of the low-temperature triclinic unit cell and is equal to 90 in the monoclinic phase. We have extrapolated the data to $T = 0$ K, and plotted the values of $\cos^2\alpha^*$ at 0 K and the transition temperatures as functions of x on the same graph, Fig. 8. It is clear from this figure that the transition behaviour is well-described by equation (2).

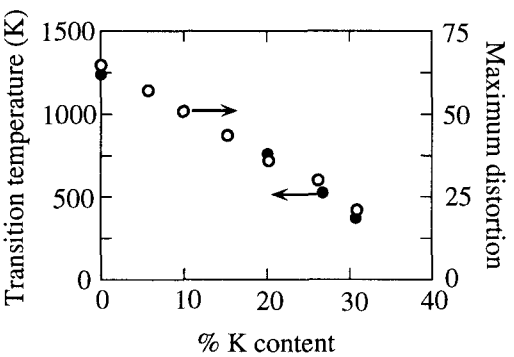

FIG. 8. The dependence of the transition temperature (closed circles, left-hand axis) and maximum distortion (open circles, right-hand axis) on K content in albite, $K_xNa_{1x}AlSi_3O_8$. The maximum distortion is equivalent to 1000 × $\cos^2\alpha^*$. Data are from Carpenter (1988).

Summary

We have sketched a number of properties of phase transitions that are explained by the RUM model. We have elsewhere outlined a number of other crystal properties for which the RUM model has applications, for example cation ordering, zeolite catalysis, and negative thermal expansion (Dove *et al.*, 1992, 1993, 1995*a*). In this paper we have sought to show how the RUM model can explain the occurrence of specific phase transitions, and how it can explain the value of the corresponding transition temperatures. The phase transitions are allowed by the existence of low-energy modes of deformation of the structure, namely without any distortion of the tetrahedra, and we have identified three different forces that can act to drive the transition or differentiate between different candidate deformations. The RUM model also provides a rationalisation for the observed transition temperatures, and we have shown the central role of the stiffness of the tetrahedra in this. The RUM model also helps explain the success of Landau theory in providing a comprehensive description of the thermodynamic properties associated with these phase transitions.

Acknowledgements

We are grateful to M Vallade (Grenoble), who introduced the RUM model of quartz to us and inspired us to generalise it for other aluminosilicates. We are also grateful to colleagues in Cambridge,

H. Deng, A. Giddy, E. Salje, P. Sollich, I. Swainson, and S. Tautz, who have contributed to this project. Our work has been supported by NERC, The Royal Society, and SERC.

References

Berge, B., Bachheimer, J.P., Dolino, G., Vallade, M. and Zeyen, C.M.E. (1986) Inelastic neutron scattering study of quartz near the incommensurate phase transition. *Ferroelectrics*, **66**, 73–84.

Bethke, J., Dolino, G., Eckold, G., Berge, B., Vallade, M., Zeyen, C.M.E., Hahn, T., Arnold, H. and Moussa, F. (1987) Phonon dispersion and mode coupling in high-quartz near the incommensurate phase transition. *Europhysics Letters*, **3**, 207–12.

Boysen, H. (1990) Neutron scattering and phase transitions in leucite. In *Phase transitions in ferroelastic and co-elastic crystals* (E.K.H. Salje, ed.). Cambridge University Press, 334–49.

Bruce, A.D.and Cowley, R.A. (1981) *Structural Phase Transitions*. Taylor and Francis, London.

Carpenter, M.A. (1988) Thermochemistry of aluminium/silicon ordering in feldspar minerals. In *Physical properties and thermodynamic behaviour of minerals* (E.K.H. Salje, ed.). Dordrecht, Holland: D. Reidel, 265–323.

Dolino, G., Berge, B., Vallade, M. and Moussa, F. (1989) Inelastic neutron scattering study of the origin of the incommensurate phase of quartz. *Physica*, **B156**, 15–16.

Dolino, G., Berge, B., Vallade, M. and Moussa, F. (1992) Origin of the incommensurate phase of quartz: I. Inelastic neutron scattering study of the high temperature b phase of quartz. *Journal de Physique, I.* **2**, 1461–80.

Dove, M.T. (1993) *Introduction to Lattice Dynamics*. Cambridge University Press, Cambridge.

Dove, M.T. and Heine, V. (1995) Anatomy of a structure phase transition: theoretical analysis of the displacive phase transition in quartz and other silicates. (in preparation).

Dove, M.T., Giddy, A.P. and Heine, V. (1992) On the application of mean-field and Landau theory to displacive phase transitions. *Ferroelectrics*, **136**, 33–49.

Dove, M.T., Giddy, A.P. and Heine, V. (1993) Rigid unit mode model of displacive phase transitions in framework silicates. *Trans. Amer. Crystallogr. Assoc.*, **27**, 65–74.

Dove, M.T., Chen, X., Giddy, A.P., Hammonds, K.D. and Heine, V. (1995*a*) Simplicity in complexity: Structural phase transitions in silicate framework structures. *Phys. Rev. Letters* (in press).

Dove, M.T., Hammonds, K.D., Heine, V., Withers, R.L., Xiao, Y. and Kirkpatrick, R.J. (1995*b*) Rigid Unit Modes in the High-Temperature Phase of SiO_2 Tridymite: Calculations and Electron Diffraction. *Phys. Chem. Minerals* (submitted).

Giddy, A.P., Dove, M.T., Pawley, G.S. and Heine, V. (1993) The determination of rigid unit modes as potential soft modes for displacive phase transitions in framework crystal structures. *Acta Crystallogr.*, **A49**, 697–703.

Grimm, H. and Dorner, B. (1975) On the mechanism of the $\alpha\beta$ phase transformation of quartz. *Phys. Chem. Solids*, **36**, 407–13.

Hammonds, K.D., Dove, M.T., Giddy, A.P. and Heine, V. (1994) CRUSH: A FORTRAN program for the analysis of the rigid unit mode spectrum of a framework structure. *Amer. Mineral.*, **79**, 1207–9.

Hammonds, K.D., Dove, M.T., Giddy, A.P., Winkler, B. and Heine, V. (1995) Rigid unit phonon modes and structural phase transitions in framework silicates. *Amer. Mineral.* (submitted).

Hatch, D.M. and Ghose, S. (1991) The α–b phase transition in cristobalite, SiO_2. *Phys. Chem. Minerals*, **17**, 554–62.

Hazen, R.M. and Finger, L.W. (1982) *Comparative crystal chemistry: temperature, pressure, composition and the variation of crystal structure*. Chichester: Wiley.

Hua, G.L., Welberry, T.R., Withers, R.L. and Thompson, J.G. (1988) An electron diffraction and lattice-dynamical study of the diffuse scattering in β-cristobalite, SiO_2. *J. Applied Crystallogr.*, **21**, 458–65.

Lasaga, A.C. and Gibbs, G.V. (1988) Quantum mechanical potential surfaces and calculations of minerals and molecular clusters. *Phys. Chem. Minerals*, **16**, 29–41.

Megaw, H.D. (1973) *Crystal structures: a working approach*. Philadelphia: W.B. Saunders.

Palmer, D.C. (1990) Volume anomaly and the impure ferroelastic phase transition in leucite. In *Phase transitions in ferroelastic and co-elastic crystals* (E.K.H. Salje, ed.). Cambridge University Press, 350–66.

Pawley, G.S. (1972) Analytic formulation of molecular lattice dynamics based on pair potentials. *Physica Status Solidi*, **49b**, 475–88.

Phillips B.L., Thompson J.G., Xiao Y. and Kirkpatrick R.J. (1993) Constraints on the structure and dynamics of the β-cristobalite polymorphs of SiO_2 and $AlPO_4$ from ^{31}P, ^{27}Al and ^{29}Si NMR spectroscopy to 770 K. *Phys. Chem. Minerals*, **20**, 341–52.

Sanders, M.J., Leslie, M. and Catlow, C.R.A. (1984) Interatomic potentials for SiO_2. *J. Chem. Soc.: Chemical Communications*, 1271–3.

Schmahl, W.W., Swainson, I.P., Dove, M.T. and Graeme-Barber, A. (1992) Landau free energy and order parameter behaviour of the ab phase transition in cristobalite. *Zeits. Kristallogr.*, **201**, 125–45.

Sollich, P., Heine, V. and Dove, M.T. (1994) The

Ginzburg interval in soft mode phase transitions: Consequences of the Rigid Unit Mode picture. *J. Phys.: Condensed Matter*, **6**, 3171–96.

Stokes, H.T. and Hatch, D.M. (1988) *Isotropy Subgroups of the 230 Crystallographic Space Groups*. World Scientific, Singapore.

Swainson, I.P. and Dove, M.T. (1993*a*) Low-frequency floppy modes in β-cristobalite. *Phys. Rev. Letters*, **71**, 193–6.

Swainson, I.P. and Dove, M.T. (1993*b*) Comment on 'First-Principles Studies on Structural Properties of β-cristobalite'. *Phys. Rev. Letters*, **71**, 3610.

Tautz, F.S., Heine, V., Dove, M.T. and Chen, X. (1991) Rigid unit modes in the molecular dynamics simulation of quartz and the incommensurate phase transition. *Phys. Chem. of Minerals*, **18**, 326–36.

Vallade, M., Berge, B. and Dolino, G. (1992) Origin of the incommensurate phase of quartz: II. Interpretation of inelastic neutron scattering data. *Journal de Physique, I.* **2**, 1481–95.

Welberry, T.R., Hua, G.L. and Withers, R.L. (1989) An optical transform and Monte Carlo study of the disorder in β-cristobalite SiO_2. *J. Appl. Crystallogr.*, **22**, 87–95.

Withers, R.L., Thompson, J.G. and Welberry, T.R. (1989) The structure and microstructure of α-cristobalite and its relationship to β-cristobalite. *Phys. Chem. Minerals*, **16**, 517–23.

Withers, R.L., Thompson, J.G., Xiao, Y. and Kirkpatrick, R.J. (1995) An electron diffraction study of the polymorphs of SiO_2-tridymite. *Phys. Chem. Minerals*, **21**, 421–33.

Wright, A.F. and Leadbetter, A.J. (1975) The structures of the β-cristobalite phases of SiO_2 and $AlPO_4$. *Phil. Mag.*, **31**, 1391–1401.

[*Revised manuscript received 15 March 1995*]